Available online at www.sciencedirect.com

ScienceDirect

Procedia Engineering 14 (2011) 185–194

Procedia Engineering

www.elsevier.com/locate/procedia

The Twelfth East Asia-Pacific Conference on Structural Engineering and Construction

# Railway Ballast Diagnose through Impact Hammer Test

H.F. Lam[a] and M.T. Wong[b,1]

[a]Department of Building and Construction, City University of Hong Kong, HKSAR, China
[b]MTR Corporation, Hong Kong

**Abstract**

This paper reports a feasibility study in the use of measured modal parameters of in-situ concrete sleepers to detect possible damage of the underlying railway ballast. There are many methods developed for monitoring and damage detection of the rail track. However, the detection of ballast damage still heavily relies on visual inspection and destructive core test. In this feasibility study, a typical plain ballasted track with concrete sleeper is considered. In the proposed method, ballast under sleeper is modelled as an elastic foundation. Ballast damage is defined as ballast degradation and ballast cementation with the accumulation of fines. When the ballast is damaged, the stiffness provided in supporting the sleeper will reduce, and the vibration characteristic of the in-situ sleeper will be altered. This paper studies the possibility to detect the damage status of ballast under a sleeper by monitoring the vibration of the corresponding sleeper through simple impact hammer test. This paper not only presented the theoretical development but also the numerical verifications.

*Keywords:* Railway Ballast; Concrete Sleeper; Damage Detection; Modal Identification; Impact Hammer Test

## 1. Introduction

Innumerable high speed railways have been constructed around the world. The mass railway transportation becomes more and more important to the development of the countries' economies and societies. Recently, new railway technologies are developing at tremendous speed. For example, China High Speed Rail achieved the world record of 350Kph and the axle load is increased over 25tonnes. Under such a heavy and repeated train loadings, the degradation of ballast is very fast. Once the train

[1] Corresponding author and presenter:
*E-mail address:* PWMSMTW@mtr.com.hk

1877–7058 © 2011 Published by Elsevier Ltd.
doi:10.1016/j.proeng.2011.07.022

speed reaches the critical train speed, the amplitude of the track vibration will be increased significantly, and cause safety problem of the railway system.

The ballasted track system is one of the most popular conventional railway track structures, which consists of the superstructure and the substructure. The superstructure contains the rails, the fastening and the sleeper, while the sub-structure contains the ballast, sub-ballast and subgrade. The ballast, which includes loose and coarse grained aggregate, supports the rails and the sleepers against vertical, lateral and longitudinal displacement. Furthermore, the ballast distributes cycle train loadings from sleeper to subgrade, provides resilience to vibration and facilitates the maintenance; provides water drainage from the track structure, retards the growth of vegetation and resists the effects of fouling from deposited materials. The size of the fresh ballast is normally 50mm. After years of services, the size of ballast will degraded to 35mm with some fines. If the maintainer does not replace the sub-graded ballast, it will be further broken down into small aggregate with less than 15mm with the fines accumulated on the track bed. In this study, ballast damage is defined as ballast degradation under heavy traffic loadings and ballast cementation with the accumulation of fines from tamping action and other loads. Ballast damage reduces not only the size of ballast but also the packing level of the ballast in certain region under sleepers and along the railway track, which results in uneven support of the railway (Selig & Waters 1997). The consequence can be with track twist and warp, and rail buckling by temperature loading creating the potential for derailment. The current solution in addressing ballast degradation is to conduct ballast cleaning and/or ballast renewal. The ballasted track quality does not really improve after renewal of damaged ballast, because there has been no reliable system of the track bed evaluation. When there is any abnormal vibration reported by the train driver or passengers, it is quite common for the permanent way engineer or inspectors to identify the problems based on their "gut feeling". Ballast damaged detection methods can be categorized into destructive and non-destructive. One of the most popular destructive methods is to dig several shallow trial pits that allow engineers or inspectors to observe the ballast condition. According to the authors' experience, this method is subjective and may not accurately identify the exact cause of problem. In the past few years four indirect non-destructive techniques have been introduced, namely Ground Probing Radar (GPR) (Narayanan et al. 2001; Roberts el al. 2007; Al-Qadi et al. 2008), Continuous Surface Wave System (CSWS) (Sutton & Snelling 1998; Moxhay et al. 2008), Falling Weight Deflectometer (FWD) (Burrow et al. 2007) and Track Geometry/Overhead Line Inspection (TOV).

The stiffness provided by the ballast in supporting a sleeper depends on the size and packing level of the ballast (Kaewunruen & Remennikov 2007). It was proved from previous studies (Lam et al. 2009; Lam et al. 2010) that ballast-damage can induce detectable changes in vibration characteristics of the in-situ sleeper. The main objective of this paper is to study the feasibility in using the vibration characteristics of in-situ concrete sleepers in quantifying the health status of ballast directly under the sleepers. A fast real-time ballast damage detection method that can be implemented by permanent way inspectors with simple equipment can certainly provide valuable information for engineers in assessing the safety and riding quality of ballasted track systems.

## 2. MODELING OF THE RAIL-SLEEPER-BALLAST SYSTEM

In this feasibility study, the sleeper is modelled as an Euler beam, and the two rails (with rail pads) on the sleeper are considered as two elastic springs with spring constant kR. The effect of ballast is represented by an elastic foundation with stiffness kB. Figure 1 shows the modelling of the rail-sleeper-ballast system. The sleeper is modelled by 24 equal-length elements for capturing the variation of cross sectional properties along the sleeper. The ballast under the sleeper is divided into six regions (see Figure

1) for the purpose of ballast damage detection. In the undamaged state, the stiffness values of ballast at all six regions are assumed to be the same.

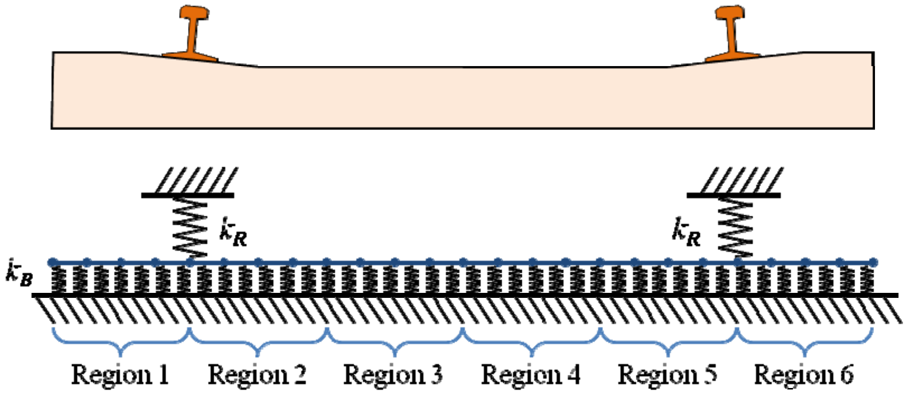


Figure 1: Modeling the rail-sleeper-ballast system

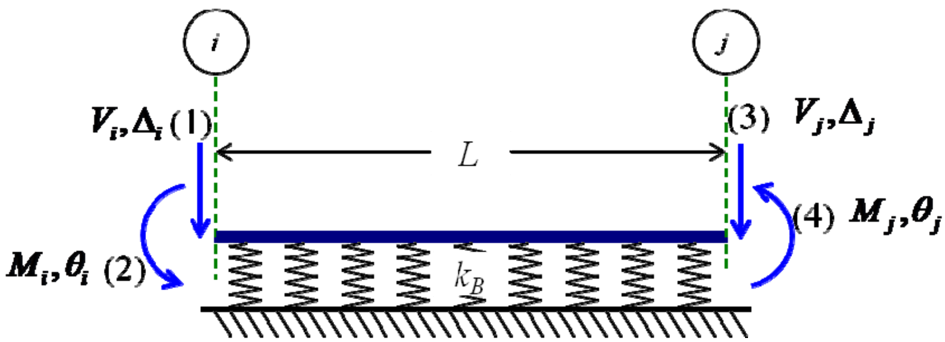


Figure 2: The Euler beam on elastic foundation element

The formulation of the element stiffness matrix of an Euler beam on elastic foundation can easily be found from the literature. In this study, the formulation from Krenk (2001) is adopted. Figure 2 shows the element employed for modelling the sleeper on ballast. The starting node is $i$ and the ending node is $j$. There are four degrees-of-freedom, two at the starting node and the other two at the ending node. The length of the element is $L$ and the stiffness of the elastic foundation is assumed to be $k_B$. The element stiffness **k** can be expressed as (Krenk 2001):

$$\mathbf{k} = \frac{EI}{L^3}\begin{bmatrix} 12\psi_1 & -6\psi_3 L & -12\psi_2 & -6\psi_4 L \\ -6\psi_3 L & 4\psi_5 L^2 & 6\psi_4 L & 2\psi_6 L^2 \\ -12\psi_2 & 6\psi_4 L & 12\psi_1 & 6\psi_3 L \\ -6\psi_4 L & 2\psi_6 L^2 & 6\psi_3 L & 4\psi_5 L^2 \end{bmatrix} \quad (1)$$

where $E$ and $I$ are the modulus of elasticity and the second moment of area, respectively, of the element; the coefficients $\psi_i$ for $i$ = 1 to 6 can be expressed as:

$$\psi_1 = \frac{1}{3}(\lambda L)^2 \psi\left[\sinh(\lambda L)\cosh(\lambda L) + \sin(\lambda L)\cos(\lambda L)\right]$$

$$\psi_2 = \frac{1}{3}(\lambda L)^2 \psi\left[\sin(\lambda L)\cosh(\lambda L) + \sinh(\lambda L)\cos(\lambda L)\right]$$

$$\psi_3 = \frac{1}{3}(\lambda L)\psi\left[\sinh^2(\lambda L) + \sin^2(\lambda L)\right]$$

$$\psi_4 = \frac{2}{3}(\lambda L)\psi \sin(\lambda L)\sinh(\lambda L)$$

$$\psi_5 = \frac{1}{2}\psi\left[\sinh(\lambda L)\cosh(\lambda L) - \sin(\lambda L)\cos(\lambda L)\right]$$

$$\psi_6 = \psi\left[\sin(\lambda L)\cosh(\lambda L) - \sinh(\lambda L)\cos(\lambda L)\right]$$

where:

$$\psi = \frac{\lambda L}{\sinh^2(\lambda L) - \sin^2(\lambda L)}, \text{ and } \lambda = \left(\frac{k_B}{4EI}\right)^{\frac{1}{4}}$$

To consider the dynamic effect, the consistent mass matrix is employed in this study (Paz & Leigh 2003):

$$\mathbf{m} = \frac{\rho AL}{420}\begin{bmatrix} 156 & 22L & 54 & -13L \\ 22L & 4L^2 & 13L & -3L^2 \\ 54 & 13L & 156 & -22L \\ -13L & -3L^2 & -22L & 4L^2 \end{bmatrix} \tag{2}$$

where $\rho$ and $A$ are the mass density and cross-sectional area of the element. Since the orientations of all elements are the same, the local coordinate system of the elements is selected to be collinear with the global coordinate system. Therefore, no transformation is required. After assembling, the system stiffness matrix **K** and system mass matrix **M** can be obtained. The natural frequencies and mode shapes of the rail-sleeper-ballast system can be calculated by solving the eigenvalue problem.

## 3. NUMERICAL CASE STUDY

In order to study the possibility of using the modal parameters of the concrete sleeper in assessing the health condition of the underlying ballast, a series of numerical case studies were carried out. In this study, a typical rail-sleeper-ballast system in Hong Kong, which consists of two UIC60 rails, a pre-stressed concrete sleeper and granite ballast, is employed. The model parameters of the rail-sleeper-ballast system employed are summarized in Table 1. Most of the model parameters are obtained from the specification from the concrete sleeper manufacturer. The values for the equivalent stiffness for the ballast and the rails are obtained from the literature (Zhai et al. 2004).

In the undamaged state, the equivalent stiffness coefficients of ballast for all 24 regions are assumed to be). The equivalent stiffness coefficients of the left and right rails are assumed to be identical (see the numerical value in Table 1).

The model predicted natural frequencies and mode shapes are summarized in Figure 3. For the comparison of mode shapes from different damage cases, the mode shapes are normalized such that the length of the mode shape vector is equal to unity. In real measurement, only the first three bending modes of the in-situ sleeper can be measured in high accuracy through impact hammer test. Therefore, only the first three bending modes of the sleeper are considered in this study.

Table 1: The set of model parameters employed in the case study.

| Model parameter (unit) | Value |
|---|---|
| The length of the sleeper, $L$ (mm) | 2420 |
| The equivalent height of the sleeper, $h$ (mm) | 210 |
| The equivalent width of the sleeper, $b$ (mm) | 280 |
| The equivalent modulus of elasticity, $E$ (N/m$^2$) | $4.0 \times 10^{10}$ |
| The density, $\rho$ (kg/m$^3$) | 2750 |
| *The equivalent stiffness provided by the ballast to the sleeper (N/m$^2$) | $7.840 \times 10^7$ |
| *The equivalent stiffness provided by the rail on the sleeper (N/m) | $2.059 \times 10^{11}$ |

* Values extracted from Zhai et al. (2004)

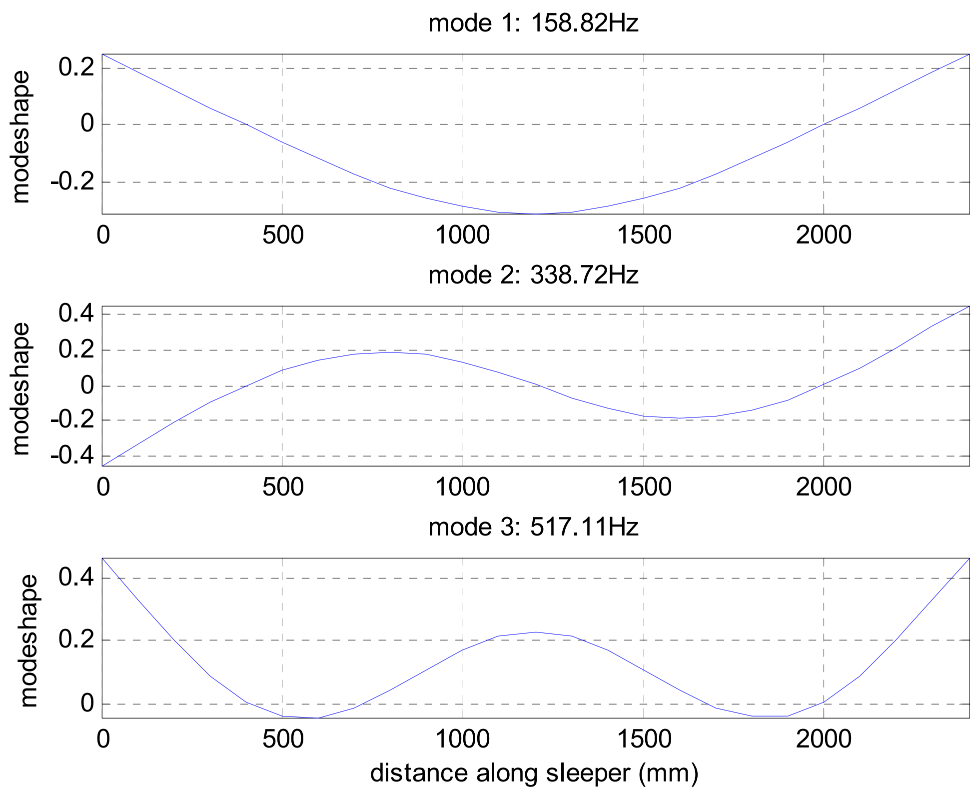


Figure 3: Model predicted natural frequencies and mode shapes of the first three modes

### *3.1. Effects of Ballast Damage on the In-situ Sleeper*

When the ballast under the concrete sleeper is damaged, the size of ballast and so as the relative packing level will be reduced. This can be simulated as the reduction in stiffness provided by the ballast to the sleeper. Note that ballast damage may result in voided concrete sleepers, and therefore, the stiffness coefficient may be reduced to a value very close to zero (near 100% reduction in stiffness) at certain regions under the sleeper. In this numerical case study, ballast damage is simulated by a 90% reduction in stiffness coefficient at the corresponding regions.

Table 2 summarizes the five cases considered and the corresponding damage location and extents. Case 1 is the undamaged case, which is used as a reference to study the effect of ballast damage on the dynamic characteristics of the system. The ballast directly under the rail is easier to be damaged when compared to the ballast under the center of sleeper due to the stress transferred from the train wheel. Therefore, Cases 2, 3 and 5 are dedicated to study this situation. Case 4 that considers ballast damage under the middle of the sleeper is also considered for the completeness of the study.

Table 2: Damage cases considered in the numerical case study

| Case | Damage location | Percentage reduction in stiffness | | | | | |
|---|---|---|---|---|---|---|---|
| | | Region 1 | Region 2 | Region 3 | Region 4 | Region 5 | Region 6 |
| 1 | Undamaged | 0 | 0 | 0 | 0 | 0 | 0 |
| 2 | At the right end | 90% | 90% | 0 | 0 | 0 | 0 |
| 3 | At the left end of sleeper | 0 | 0 | 0 | 0 | 90% | 90% |
| 4 | At the middle of the sleeper | 0 | 0 | 90% | 90% | 0 | 0 |
| 5 | At the two ends | 90% | 90% | 0 | 0 | 90% | 90% |

By computer simulation, the natural frequencies and mode shapes of the first three modes for different damage cases were calculated, and the model predicted natural frequencies and the corresponding percentage reduction for all damage cases were summarized in Table 3. It is clear from the table that ballast damage reduces the natural frequencies in all damage cases, as expected. One important observation is that the percentage reductions in natural frequencies are different for different modes and different damage cases. In other words, the changes in natural frequencies do contain information about the location and extent of ballast damage.

For Case 2, the changes in natural frequencies are larger than 2% for modes 1 (4.45%) and 2 (2.1%), but it is less than 1% for mode 3 (0.73%). It is clear that modes 1 and 2 are more sensitive to the ballast damage in this case, while mode 3 is relatively insensitive.

It must be pointed out that natural frequencies are global properties of the system. Since the rail-sleeper-ballast system considered in this case study in its undamaged state is symmetrical about the center, symmetrical ballast damage cases will induce the same changes in natural frequencies. Therefore, the changes in modes 1, 2 and 3 natural frequencies for ballast damage under the left and right rails (i.e. Cases 2 and 3) are the same.

For Case 4, mode 1 is very sensitive (18.84%), while modes 2 and 3 are not. For Case 5, mode 1 is the most sensitive one and mode 2 is not as sensitive to mode 1, and mode 3 is the most insensitive one. It is clear that different modes will have different sensitivities to damage at different location. Figure  plots the percentage changes in natural frequencies of the first three modes in all damage cases. It can be observed from the figure that different damage cases reduce the natural frequencies in different patterns. It is possible to use these patterns for the purpose of ballast damage detection following the pattern matching approach (Lam & Ng 2008). With the advance in measurement equipment, natural frequencies of sleeper can be measured highly accurately with less than 1% error. Therefore, a percentage change of larger than 1% can be considered as detectable. Based on the results from the numerical case study, it can be concluded that it is possible to detect the ballast damage by interpreting the damage-induced changes natural frequencies of the in-situ sleeper.

Table 3: Calculated natural frequencies for all cases.

| Case | Mode 1 | Mode 2 | Mode 3 |
|---|---|---|---|
| 1 | 158.82 | 338.72 | 517.11 |
| 2 | 151.76 (4.45%) | 331.59 (2.10%) | 513.31 (0.73%) |
| 3 | 151.76 (4.45%) | 331.59 (2.10%) | 513.31 (0.73%) |
| 4 | 128.9 (18.84%) | 335.81 (0.86%) | 513.81 (0.64%) |
| 5 | 144.97 (8.72%) | 324.26 (4.27%) | 509.34 (1.5%) |

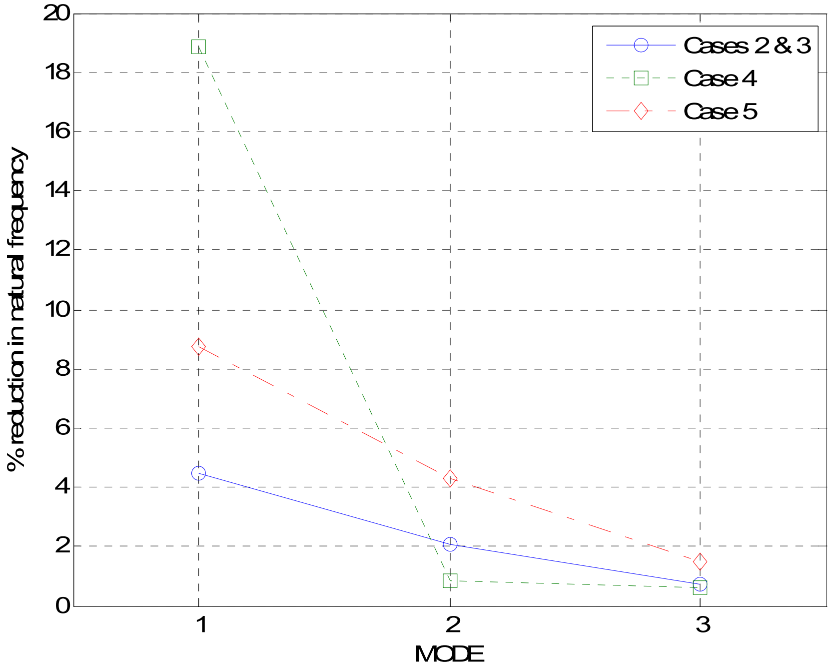


Figure 4: The use of damage-induced reduction in natural frequencies as pattern feature for damage detection

Figure  plots the calculated mode shapes of the first three modes in all Cases. It is clear from the figure that the damage-induced changes in mode shapes of the first three modes are very small. The usual percentage error for measured mode shape is about 2% to 5%, and therefore, the use of measured mode shapes of in-situ sleeper for the purpose of damage detection is not easy. Nevertheless, the measured mode shapes are very important in identifying modes.

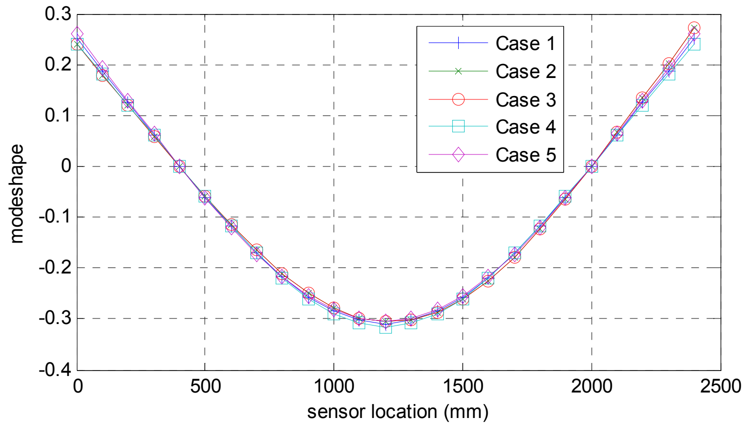


(a) mode 1

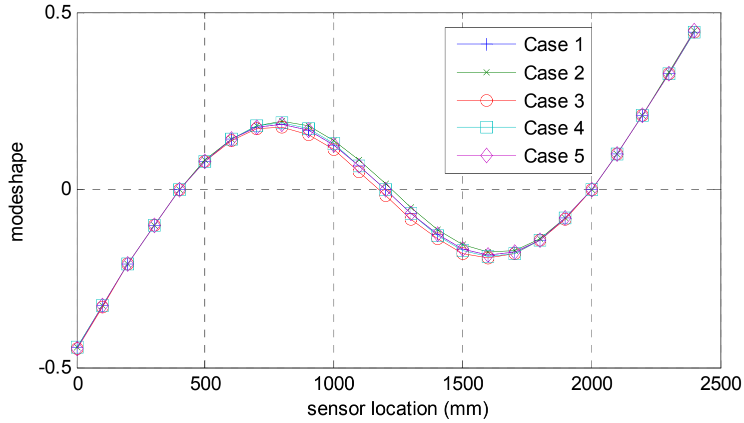


(b) mode 2

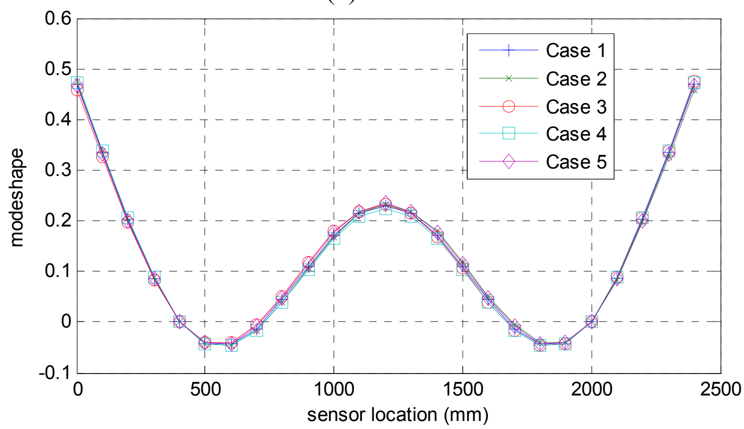


(c) mode 3

Figure 5: Calculated mode shapes of the first three modes in all cases

## 4. CONCLUSIONS

This paper reports on the feasibility study on the use of measured vibration of in-situ concrete sleeper in detecting the damage of underlying ballast. The numerical case study results are very encouraging showing that the vibration data of the in-situ sleeper does contain information about the ballast that is directly under the sleeper. In other words, it is possible to identify ballast damage through impact hammer test of the in-situ sleeper. However, many difficulties must be overcome before this approach can be applied in a real situation. First of all, the vibration measurement of sleepers at the undamaged state of the system is usually unavailable. The permanent way inspector can only measure the dynamic responses of sleepers on possibly damaged ballast on site. Note that this is a common problem in Structural Health Monitoring (SHM), and a possible solution is to develop a model (analytical or numerical) to represent the undamaged state of the rail-sleeper-ballast system. Another difficulty in the implementation of this approach is the uncertainty problem. Unlike structural systems for aerospace and mechanical systems, the model parameters of a rail-sleeper-ballast system are relatively uncertain. Probability theory should be employed in explicitly addressing the uncertainty problem. Furthermore, there are many factors affecting the vibration characteristic of in-situ sleepers, such as the damage of the sleeper itself, the rail defects and rail pads damage, and environmental factors like temperature and humidity. Those factors must be considered in the development of a practical ballast damage detection method. Nevertheless, this approach can be easily extended to a continuous monitoring system in future by installing sensors on selected sleepers in the target track system. The measured signals are transferred through communication lines along the track to the control center.

### Acknowledgments

The work described in this paper was fully supported by a grant from the Research Grants Council of the Hong Kong Special Administrative Region, China [Project No.: CityU 115510].

### References

[1] Al-Qadi IL, Xie W and Roger R (2008), Scattering analysis of ground-penetrating radar data to quantify railroad ballast contamination, NDT&E International, 41: 441-447.

[2] Burrow MPN, Chan AHC and Shein A (2007), Deflectometer-based analysis of ballasted railway tracks, Proceedings of the Institution of Civil Engineers, Geotechnical Engineering, 160, July 2007, Issue GE3: 169-177.

[3] Kaewunruen S and Remennikov AM (2007), Effect of improper ballast packing/tamping on dynamic behaviours of on-track railway concrete sleeper, International Journal of Structural Stability and Dynamics, 7(1): 167-177.

[4] Krenk S (2001), Mechanics and Analysis of Beams, Columns and Cables – A Modern Introduction to the Classic Theories, Second Edition, Springer.

[5] Lam HF and Ng CT (2008a, The Selection of Pattern Features for Structural Damage Detection Using an Extended Bayesian ANN Algorithm, Engineering Structures, 30(10): 2762-2770.

[6] Lam HF, Wong MT and Keefe RM (2009), Detection of Ballast Damage by In-situ Vibration Measurement of Sleepers, 2nd International Symposium on Computational Mechanics (ISCM II), 30 November 2009 – 3 December 2009, Hong Kong and Macau.

[7] Lam HF, Wong MT and Keefe RM (2010), Detection of Railway Ballast Damage by In-Situ Vibration Measurement of Concrete Sleepers, The 14th Annual Conference of HKSTAM 2009/2010 and The 7th Shanghai-Hong Kong Forum on Mechanics & Its Application, March 13, 2010, Hong Kong.

[8] Moxhay AL, Tinsley RD and Redgers JD (2008), The prediction of ground settlement from continuous surface wave data, Ground Engineering magazine, July 2008, pp 34-37.

[9] Narayanan RM, Kumke CJ and Li D (2001), Railroad Track Substructure Monitoring Using Ground Penetrating Radar (GPR), Rail International, 32(1): 28-34.

[10] Paz M and Leigh W (2003), Structural Dynamics: Theory and Computation, Fifth Edition, Springer.

[11] Roberts R, Al-Qadi IL, Tutumluer E and Kathage A (2007), Ballast fouling assessment using 2 GHz horn antennas - GPR and ground truth comparison from 238 km of track, 9th International Railway Engineering Conference (London, UK, Jun. 2007). (Download: http://www.alphageofisica.com.br/gssi/gpr_2008/RailEng%202007_br.pdf)

[12] Selig ET and Waters JM (1997), Track Geotechnology and Substructure Management, Thomas Telford.

[13] Sitharam TG and Anbazhagan P (2006), Measurements of Dynamic Properties and Soil Profiling Using Multichannel Analysis of Surface Waves, Invited Keynote in 4th Karl Terzaghi Memorial Workshops, October07, 2006 at Madgaon, Goa, P-6.

[14] Sutton JA and Snelling K (1998), Assessment of Ground Improvement Using the Continuous Surface Wave Method, Proceedings of the 4th Meeting of the Environmental and Engineering Geophysical Society, Barcelona, 14-17th September 1998.

[15] Zhai WM, Wang KY and Lin JH (2004), Modelling and experiment of railway ballast vibration, Journal of Sound and Vibration 270(9): 673-683.